Environment

Attachment strength of seed mucilage prevents seed dislodgement in high surface flow: a mechanistic investigation

Vincent S. Pan[1,2,3], Cecilia Girvin[1], Eric F. LoPresti[1]

1: Department of Plant Biology, Ecology, and Evolution, Oklahoma State University, 421 Physical Sciences, Stillwater, Oklahoma 74078

2: Department of Integrative Biology, Michigan State University, 288 Farm Lane, East Lansing, Michigan 48824

3: Corresponding Author: vsbpan@gmail.com

Key words

Antitelechory, Erosion, Myxodiaspory, Seed functional traits, Seed mucilage

Author contributions

VSP, CG, & EFL designed the study, collected the data, and made the figures. VSP conducted the analysis. VSP & EFL wrote the manuscript. CG provided editorial support.

Conflict of interest

We declare no conflict of interest.

Data availability statement

All data and code used to generate this manuscript are available on Dryad and Zenodo respectively: https://doi.org/10.25338/B81M00

Abstract

1. Seed mucilage is a common and highly diverse trait shared among thousands of angiosperms. While long recognized that mucilage allows seeds to anchor to substrates (antitelechory), we still lack a mechanistic understanding of this process.
2. We propose a mechanistic model of how mucilage affects substrate anchorage and fluid resistance, ultimately contributing to antitelechory. To test this model, we subjected mucilaginous seeds of 52 species, varying in eight measured seed traits, to a week of continuous water flow at a range of erosion potentials.
3. Supporting our model, mucilage mass increased both dry and wet attachment strength, which explained time to erosion well. A standard deviation increase in log mucilage mass increased seed time to dislodgement by 280 times. Fluid resistance was largely dependent on speed of water flow and the seed's modified drag coefficient, but not the quality of the seed or seed mucilage. Neither mucilage expansion speed nor mucilage decay rate explained dislodgement potential well.
4. Our results suggest that the high substrate anchorage strength is the primary role of mucilage in fostering seed establishment in highly erosive environments. In contrast, other seed and mucilage trait differences among species are of lesser importance to antitelechory.

Introduction

Diaspore mucilage (myxodiaspory, hereafter: seed mucilage) is an extremely widespread trait in plants with thousands of species across monocots and dicots (Grubert, 1974, 1981). When wetted, mucilage-secreting cells absorb water and swell up, eventually releasing a complex matrix of hydrated cellulosic, pectic, and hemicellulosic sugars (Grubert, 1974, Western, 2012, North et al., 2014). This matrix may be sticky or slippery when wet, but after drying, generally anchors seeds to substrates tightly (Kreitschitz et al., 2021b, Pan et al., 2021). Previous workers have observed its utility in anchorage (i.e. antitelechory) and noted its ubiquity among plants in highly erosive environments (Ellner & Schmida, 1981, Garcia-Fayos et al., 2013), and have experimentally demonstrated its role in antitelechory in two species of Cistaceae (Engelbrecht et al., 2014). Since seed mucilage is an amalgamation of measurable traits— chemical composition, structure, volume, and physical properties of both the mucilage envelope and seed (Grubert 1974, Western, 2012, Kreitschitz & Gorb, 2018, Viudes et al., 2020, Cowley & Burton, 2020)— functional investigations across species can provide a mechanistic understanding of how this anchorage occurs and what trait combinations might have the highest antitelechorous potential.

In the few studies which have examined across species or populations, specific mucilage traits have been predictive of functional or ecological performance. In Pan et al. (2021), species with stronger anchorage were more protected from granivorous ants, as were seeds with more mucilage-bound sand (LoPresti et al., 2019). In the only example explicitly dealing with antitelechory, Engelbrecht et al. (2014) found that seeds of *Fumana ericoides* (Cistaceae) from low erosion sites produced significantly less mucilage than those from high erosion sites; suggesting functional variation in the trait, though another species in the same family (*Helianthemum violaceum*) did not show the same pattern. Much excellent experimental research

on the ecological functions of mucilage in relation to dispersal, germination, defense, and stress amelioration (e.g. Fuller & Hay, 1983, Huang et al., 2008, 2015, Kreitschitz et al., 2021a, Zhao et al., 2021) has been done, but only with one or a few species. Therefore, while we know many functional roles of mucilage in certain species, we do not know how specific aspects of mucilage contribute to these roles.

As mucilage traits vary both within and across species, determining the functional roles of this variation can provide insight into the evolutionary pressures shaping these traits. When looking broadly, mucilage mass and attachment potential measured across 53 plant species in LoPresti et al. (2019) and Pan et al. (2021) were strongly correlated among closer related species. However, when looking in-depth at close relatives, there is often much variation. Comparisons of many *Plantago* species reveals a wide variety of mucilage morphology across the genus (Cowley & Burton, 2021, Cowley et al. 2021) as does examining variation across populations of other widespread species or genera (e.g. Kreitschitz & Vallès, 2007, Inceer et al., 2012; Villellas & Garcia, 2012, Engelbrecht et al., 2014, Poulain et al., 2019, Teixeira et al., 2020). Therefore, understanding mechanistic consequences of this variation is of paramount importance in interpretation of these documented patterns.

Across plants, particularly from desert or ruderal environments, myriad traits prevent primary or secondary dispersal and these traits are especially important in preventing dislodgement and transport into unsuitable habitat (Ellner & Schmida, 1981, Garcia-Fayos et al., 2013, Engelbrecht et al., 2014). Staying in place likely provides several advantages in many habitats. Seeds may avoid becoming badly abraded in the erosion process or the risk of burial with lower chance of emergence (Mennan & Zandstra, 2006). In environments where other plants are continuously filtered by erosion, the remaining plants may face little to no

47 competition, in contrast to areas where seeds collect after erosion in high numbers. The lower
48 plant density also likely meant that there is lower pressure from disease (Bell et al., 2006) and
49 herbivory (Kim & Underwood, 2015). Thus, antitelechory mechanisms may be seen as essential
50 traits for certain plants to uniquely exploit highly erosive niches. For annuals especially,
51 antitelechory may be important for continued occupation of suitable patches during the seed
52 stage (Grubert et al., 1974, Ryding, 2001, Pan et al., 2021). However, these assertions are not
53 meant to suggest that dispersal is not favorable in many instances; instead, the suites of traits that
54 promote antitelechory are repeatedly evolved, and therefore, likely favorable in certain contexts
55 (Ellner & Schmida, 1981).

56 Rainfall, and subsequent surface flow across steep slopes is a common type of
57 dislodgement that is directional and may be responsible for staggering seed mortality. Han et al.
58 (2011) found that 60-90% of seeds experimentally placed on shallow slopes were washed away
59 in a single hour of heavy rain; similar results were reported by Aerts et al. (2006) who further
60 found that the effect was most pronounced on bare slopes without leaf litter (neither used any
61 mucilaginous seeds in their studies). A single, eight-hour rainfall event totaling 44 mm in a 60-ha
62 watershed in Laos was estimated to have washed 1.34 million seeds into a river due to surface
63 flow, estimated to be >1% of all seeds in the area (de Rouw et al., 2018). Given that the area
64 receives 1403 mm of precipitation annually (de Rouw et al., 2018), this sort of flow could
65 disperse or cause mortality to a large fraction of seeds produced each year. We know of no
66 comparable estimates for other areas, but this sort of dislodgement is certainly a risk to seeds in
67 many, if not all, habitats, and could represent powerful selective force on antitelechorous traits
68 (Ellner & Schmida, 1981, Garcia-Fayos et al., 2013, Engelbrecht et al., 2014).

Imbibed seed mucilage binds seeds strongly to whatever it contacts, be it loose substrate, hard-packed substrate, rocks, leaves, or the mother plant itself as it dries (Pan et al., 2021). Mucilage has been documented to anchor seeds strongly against runoff in the field (*Plantago ovata*, Plantaginaceae: Ellner & Schmida, 1981) and laboratory (*Helianthemum violaceum* and *F. ericifolia*, Cistaceae: Engelbrecht et al., 2014). The anchorage strength of mucilage after a wetting-drying cycle is extremely strong and correlates positively with the amount of mucilage produced (Kreitschitz et al., 2021b, Pan et al., 2021). Wet mucilage is still sticky, which is important for zoochorous dispersal (Ryding, 2001), but the strength of attachment is considerably lower than after drying and has not been well characterized besides in flax, *Linum usitatissimum* (Kreitschitz et al., 2015). In the face of surface flow, the speed at which mucilage rehydrates, switching from stronger to weaker attachment, may thus contribute to the length of time that substrate anchorage is effective. Over longer periods, the breakdown of the mucilage layer in water may also reduce the amount of mucilage or strength of mucilage attachment, lowering resistance to dislodgement. Seed mucilage may further alter the fluid resistance in complex ways. The expansion of the mucilage envelope provides a larger area upon which flowing water may exert force on. However, some of the drag may be alleviated by the improvement in sphericity for more rigid mucilage envelopes or closer resemblance to a streamlined shape for more malleable mucilage envelopes in fast flowing water. In addition, lubrication provided by the mucilage layer between water and seed may reduce the force that is exerted on the seed.

Integrating these functional hypotheses, we propose a multi-part model for the physical mechanisms underlying antitelechory in mucilaginous seeds (Figure 1, 2). Specifically, we work under the framework of the two major mechanistic processes, the ability of seeds to withstand

92 horizontal shear force and the amount of shear force the seeds experience as a result of fluid
93 resistance. Contributing to the attachment potential is the amount of mucilage, the rate at which
94 that mucilage expands, the rate it decays, and the seed size. Contributing to drag is seed size
95 (including imbibed mucilage), the mucilage decay and expansion rate, and seed shape.
96 Externally, the intensity of surface flow also contributes to potential for successful antitelechory.
97 In this study, we tested the proposed physical model with mucilaginous seeds of 52
98 species in varying intensities of erosive surface flows. We examined how each seed trait relates
99 to substrate attachment potential for the ability to withstand shear force and to projected area
100 (largest cross-sectional area) and drag coefficient for fluid resistance. We characterized seed
101 mass, seed mucilage mass, and two temporal aspects of mucilage quantity in water (i.e. speed of
102 mucilage expansion and breakdown). After identifying useful predictors of dislodgement
103 potential, we compared the marginal predictive utility of the functional assays to provide
104 guidance on future functional investigations.
105
106 **Methods**
107 *Dislodgement resistance experiment*
108 We experimentally tested whether seed mucilage facilitates anchorage during erosive
109 surface flow for 52 species of mucilaginous-seeded plants from 10 families (Table S1, Figure
110 S1). The species were selected haphazardly based on availability from commercial seed sources,
111 our field collections, or the USDA Germplasm Resources Information Network program
112 (USDA-ARS, 2015). Preliminary experiments in the field (see supplement) suggested that seeds
113 can remain stuck to inclined sandstone, vertical clay cliffs, and frequently flooded riverbanks
114 during several rainstorms (Figure 3A, D-E). To mimic the erosive effect of surface flow during

these rainstorm events, we developed a simple laboratory assay that subjected anchored seeds to a range of surface flow rates that seeds may encounter in the field (Figure S2). Seeds were imbibed in water for at least one hour, during which the mucilage of most species was able to fully expand (the average time to full expansion was 32 minutes). We placed one seed of each species inside individual divots on the back side of each ceramic tile (10 × 10 cm Hudson Brilliant White Glossy Ceramic Wall Tile) in a predetermined randomized order, then allowed the seeds to dry overnight. To present different conditions, alternating tiles were oriented right side up or upside down. We attached each tile in its predetermined orientation to a 10.5 × 10.5 × 12.5 cm plastic flowerpot with the bottom cut out, which acted as a funnel, and mounted on a 45° incline < 15 cm below individual water faucets. We turned each faucet on to a constant flow rate between 6.7×10^{-5} - 1.4×10^{-2} L/s/cm. The flow from each faucet was measured at the beginning and end of each trial, as pressure changed based on other building users; the mean of the two values was recorded as the flow speed treatment. The trials began when water started flowing and ended after either six or seven days. Each tile was monitored continuously for the first 15 minutes, on an hourly basis for the next five hours, and two to five times a day subsequently, during which we recorded the timing of each observed seed dislodgement. We used at most ten sinks simultaneously and ran the experiment over the span of two weeks for a total of 20 trials. One seed in one trial (*Leptosiphon* 'hybrid') was excluded due to a missing dislodgement time.

Functional trait assays

In order to evaluate our hypothesized mechanisms of antitelechory, we measured a variety of morphological and functional traits of seeds. We measured dry seed mass for each species by weighing several seeds together and taking the mean for a single seed; this measurement was repeated twice per species. For each species, we also estimated the individual

volume and mean projected area of four fully imbibed seeds for each species using a digital microscope (DinoCapture 2.0) by measuring the diameter of the three principal axes (see supplement). The dry dislodgement force was measured for 7-28 individual seeds/species using a modified method from Pan et al. (2021). We attached imbibed seeds to glass slides instead of adding water to dry seeds on petri dishes, which improved consistency and precision over our previous method. We also standardized the seed orientation, only pressing the Pesola spring scale perpendicularly against the long axis of the seed. Because the slipperiness of wet mucilage was not amenable to the same method, the dislodgement force of seeds when mucilage was wet was measured using a modified double-sided lever balance that pulled imbibed seeds apart from two pieces of filter paper (see supplement; Figure S3). For this assay, we measured each species three times, each time using five seeds.

We characterized the quantity of mucilage produced by different species and the temporal dynamics of mucilage quantity in water. For short term dynamics, we measured the mass of imbibed seeds of each species at roughly 0.5, 2, 8, 32, 120, 480, and 1200 minutes after wetting. We weighed four seeds at each time point, discarding seeds after weighing as their mucilage structure may have been damaged during handling. For each species at each time point t, we found the mean species mucilage mass (m) by subtracting the mean species wet mass by the mean species dry seed mass. Then, using (1), modeled after Darcy's law of hydrodynamic flow (supplemental method for derivation), we estimated mucilage mass of a fully imbibed seed (m_{max}, which is functionally equivalent to mucilage mass after 1 hour for nearly all species) and the speed coefficient of mucilage secretion in s^{-1} (a):

$$m(t) = m_{max} - m_{max}e^{-at} \quad (1)$$

We repeated the assay a few times for species which had large posterior credible intervals around the estimated parameters.

To characterize the mucilage decay over longer time periods, we weighed four different seeds every day for a week for each species. Twenty-eight seeds of each species were imbibed in 40 mL of water at 1 °C to which we added two drops of 1% bleach to prevent seed germination and decomposition. We estimated the rate of mucilage dissolution with (2):

$$m(t) = m_{max} e^{-Dt} \quad (2)$$

where $m(t)$ is the mass of mucilage at time t, m_{max} is the maximum mucilage mass, D is the mucilage decay rate coefficient in days^{-1}.

We further estimated a modified drag coefficient in water through a terminal velocity assay (Loudon & Zhang, 2002). In a 17 × 90 cm transparent cylinder filled to the brim with water at rest, we dropped imbibed seeds from the top and measured the time it took for each seed to travel 60 cm. We repeated this assay ten times for each species. All seeds reached terminal velocity within the first ten centimeters of dropping distance, hence they were measured from 20 to 80 cm below the dropping point. From the equation for objects traveling at terminal velocity, we isolated an experimental constant (k_d) that is in essence equivalent to the drag coefficient, but with the dependency on terminal velocity factored out (see supplement for derivation).

$$k_d = \frac{2g(m_{total} - \rho V_{total})}{\rho v^{(2+\beta_1)} A} \quad (3)$$

Here, g is the acceleration due to gravity, m_{total} is the mass of the seed with mucilage, ρ is the density of water, V_{total} is the volume of the imbibed seed with mucilage, β_1 is a conversion constant that relate the drag coefficient to Reynolds number, A is the projected area, and v is the terminal velocity of the seed. All parameters that we did not directly measure (m_{max}, a, D, and k_d)

were estimated using individual species linear or non-linear models with moderately regularizing priors.

Components of antitelechory

All continuous variables besides D, k_d, seed mass, and time to dislodgement were log transformed to improve linearity and all continuous predictors were standardized as Z-scores. Unsupported interactions were dropped, and the models refitted. All statistical analyses were conducted using R (version 4.0.5; R Core Team 2020). All models were constructed using the Stan interface package *brms* (Bürkner, 2017, 2018) or *rstanarm* (Goodrich et al., 2020). All cross-validations were done using the package *loo* (Vehtari et al., 2017, 2019).

We first characterized the extent to which time to dislodgement was affected by a seed's attachment to substrate and the degree of drag it experienced. We analyzed the time to dislodgement of each seed in a log-normal accelerated failure time (AFT) multilevel model (n = 1039 seeds). Tile orientation, flow speed, wet dislodgement force, dry dislodgement force, mean projected area, and the experimental drag constant k_d were included as fixed effects. Flow speed was allowed to interact with wet and dry dislodgement force, mean projected area, and k_d to test whether these processes have different effect sizes in different flow intensities. We also included mucilage decay D and mucilage wetting speed a as fixed effects and allowed them to interact with force and k_d as the temporally variable quantity of mucilage might moderate the effect of force and k_d. To take into account the uncertainty in estimated values of k_d, a, and D, we performed multiple imputations at the species level using standard errors associated with each measurement. Individual tiles and species were included as random group intercepts. In order to account for some unmeasured variables shared among close relatives that affect the results, we performed a phylogenetic correction using a Brownian correlation structure. We constructed this

matrix from a species level tree pruned from a synthesis of the most recent mega-phylogenies (Zanne, et al. 2014, Smith & Brown, 2018, *package*: *V.PhyloMaker* Jin & Qian, 2019). Unresolved species were assigned as polytomies at the genus basal node (Qian & Jin, 2016). R^2 was computed using equation three from Gelman et al. (2019) with and without group-level effects.

Contributions of seed and mucilage traits to components of antitelechory

To understand how seed and mucilage traits contribute to mechanistic component of fluid resistance and anchorage ability, we analyzed mean species dry dislodgement force, wet dislodgement force, mean projected area, and k_d in four linear models as the response variable (n = 52). Dry seed mass and max mucilage mass m_{max} were included in all models as fixed effects. Mucilage decay and an interaction with m_{max} were included in the models for wet dislodgement force and k_d. Phylogenetic relationship was specified in all models as a correlation matrix. Measurement error multiple imputations were again conducted for variables we did not directly measure (m_{max}, a, D, and k_d).

Structural equation model

We performed a piecewise confirmatory path analysis to characterize the relative magnitude and direction of how seed functional traits mechanistically contributed to antitelechory. Our structural equation model (SEM) was composed of five sub-models: four linear models for 1) wet dislodgement force, 2) dry dislodgement force, 3) mean projected area, and 4) k_d that followed the same model structure as above, in addition to 5) an average species AFT model. We condensed individual seed level time to dislodgement into mean time to dislodgement for each species as the destructive nature of our trait assays necessitated that we only had mean species level trait data. Mean time to dislodgement for each species at mean flow

speed was predicted from an AFT multilevel model as before, following the same model structure, but with only flow speed and tile orientation as fixed effects. Due to computational limitations, we limited multiple imputations to predicted dislodgement time and k_d. Plausible alternative paths were checked by including each path in a new model and comparing the leave one out information criterion (*LOOIC*). Plausible alternative paths were rejected when the decrease in *LOOIC* was < 2.

Marginal utility of functional assays

Finally, in order to determine what traits are most important to measure if time and resources are limited (for instance, in broad community functional trait studies), we characterized the marginal predictive value of different seed functional traits in understanding antitelechory. Based on the results of our path analysis and regression models, we selected five useful seed traits (mean projected seed area, seed mass, k_d, wet, and dry force) for forward model selection. We began with an AFT multilevel model of individual seed erosion time as before but with only flow speed and tile orientation as fixed effects. Variables were selected based on grouped-13-fold cross-validation information criterion; each refit of the model left four species out of sample at a time (Roberts et al., 2017).

Results

Components of antitelechory

We found strong evidence that wet and dry dislodgement force and drag force were mechanistically driving the time to dislodgement (*Conditional* R^2 = 0.71, 95% *Credible interval* (CI_{95}) = [0.68, 1.0], *Marginal* R^2 = 0.61, CI_{95} = [0.53, 1.0]). Seeds on average remained on tiles for 5.3 days, although the time to dislodgement was highly variable among flow rates and among

248 species. A standard deviation in the time to dislodgement spanned over two orders of
249 magnitudes. The ability for seeds to anchor to substrates substantially increased resistance to
250 dislodgement under surface flow (Figure 4A-B). One *SD* increase in log dry dislodgement and
251 log wet dislodgement force of seeds was associated with a 2900% (β = 3.4 ± 0.74, CI_{95} = [1.9,
252 4.8]) and 630% increase in time to dislodgement respectively (β = 1.8 ± 0.68, CI_{95} = [0.50, 3.2]).
253 Flow intensity did not affect the efficacy of either dry (β = -0.21 ± 0.26, CI_{95} = [-0.74, 0 .30]) or
254 wet force (β = 0.32 ± 0.27, CI_{95} = [-0.21, 0 .84]).

255 Variables that contributed to higher drag decreased time to dislodgement. The negative
256 effect of the modified drag coefficient was strongest at lower flow intensities ($\beta_{interaction}$ = 0.41 ±
257 0.19, CI_{95} = [0.057, 0.79]; Figure 5). At the 25th and 75th percentile flow speed, an *SD* higher k_d
258 was associated with an 84% and 44% reduction in time to dislodgement respectively (β_{kd} = -1.2 ±
259 0.65, CI_{95} = [-2.5, 0.084]). Flow speed had a negative effect on time to dislodgement regardless
260 of k_d (β_{flow} = -1.8 ± 0.32, CI_{95} = [-2.4, -1.1]). An *SD* higher flow speed reduced time to
261 dislodgement by 83% when k_d was held at average. Mean projected seed area did not have a
262 significant effect on time to dislodgement (β = -0.57 ± 0.78, CI_{95} = [-2.1, 0.96]) or interact with
263 flow speed (β = -0.40 ± 0.27, CI_{95} = [-0.92, 0.14]). In contrast to our hypotheses, neither wetting
264 speed (a) or mucilage decay (D) affected time to dislodgement (β_D = -0.55 ± 0.72, CI_{95D} = [-1.9,
265 0.96]; β_a = 0.49 ± 0.83, CI_{95a} = [-1.2, 2.1]), or interacted significantly with wet force (β_D = 0.55 ±
266 1.1, CI_{95D} = [-1.8, 2.4]; β_a = -0.50 ± 0.93, CI_{95a} = [-2.3, 1.4]), dry force (β_D = 0.054 ± 1.1, CI_{95D} =
267 [-2.2, 2.3]; β_a = 0.44 ± 1.0, CI_{95a} = [-1.5, 2.4]), or the drag coefficient, k_d (β_D = 0.82 ± 1.7, CI_{95D}
268 = [-3.9, 2.9]; β_a = 0.077 ± 0.83, CI_{95a} = [-1.6 1.6]).

Some seeds germinated during the trial. Dislodgement of the seedling post-germination occurred in 1% of seeds (11/1039) and a reanalysis, counting these germinated seeds as not dislodged, yielded results that were within rounding error from those presented here.

Contributions of seed and mucilage traits to dislodgement force

Mucilaginous seeds anchored strongly to substrates, both after a wetting-drying cycle (dry attachment) and while mucilage was fully imbibed (wet attachment). Although the method of measurement was different, the dislodgement force greatly depended on the hydration status of the mucilage. The dislodgement force of mucilage to glass slides when dry averaged 0.13 N, while the dislodgement force of wet mucilage to filter paper averaged 0.0043 N. The amount of mucilage that seeds produced correlated well with the strength of substrate anchorage for both when the mucilage was dry (β = 2.3 ± 0.24, CI_{95} = [-1.9, 2.8]) and wet (β = 0.86 ± 0.13, CI_{95} = [0.61, 1.1]) (Figure 4C-D). A one *SD* increase in log mucilage mass was associated with a 900% and 140% increase in dry and wet dislodgement force respectively. Higher seed mass was significantly correlated with lower dry dislodgement force (β = -0.72 ± 0.30, CI_{95} = [-1.3, -0.14]), but not wet dislodgement force (β = -0.023 ± 0.15, CI_{95} = [-0.33, 0.25]). Faster mucilage decay was positively correlated with higher wet dislodgement force (β = 0.65 ± 0.17, CI_{95} = [0.38, 1.0]) and its effect did not depend on the amount of mucilage (β = -0.17 ± 0.17, CI_{95} = [-0.52, 0.15]). A one *SD* increase in the rate of mucilage decay corresponded to a 92% higher wet dislodgement force. Together, these variables accounted for most of the variation in dry dislodgement force (R^2 = 0.71, CI_{95} = [0.63, 0.77]) and wet dislodgement force (R^2 = 0.76, CI_{95} = [0.65, 0.85]).

Contributions of seed and mucilage traits to drag coefficient and projected area

Mean projected area of imbibed seeds was significantly associated with higher amount of mucilage produced, independent of seed size. A one *SD* increase in log mucilage mass was

292 associated with 90% higher mean projected area (β = 0.64 ± 0.068, CI_{95} = [0.51, 0.77]). Seed
293 mass was correlated positively with mean projected area, but the association was only marginally
294 significant (β = 0.15 ± 0.086, CI_{95} = [-0.020, 0.32]). Together, both variables explained most
295 variation in mean projected area (R^2 = 0.89, CI_{95} = [0.84, 0.92]). Our modified drag coefficient k_d
296 averaged 0.9, with some estimates extending into the negative domain as seed volumes were
297 likely generally overestimated. Seed mass (β = 0.34 ± 0.49, CI_{95} = [-0.60, 1.3]), mucilage mass
298 (β = 0.19 ± 0.38, CI_{95} = [-0.57, 0.94]), the rate of mucilage decay (β = 0.00070 ± 0.0078, CI_{95} =
299 [-0.015, 0.016]), and an interaction between the rate of mucilage decay and mucilage mass did
300 not explain k_d (β = -0.015± 0.015, CI_{95} = [-0.043, 0.014]).

301 *Structural equation model*

302 The best SEM is shown in Figure 6A. We found strong evidence that higher mucilage
303 mass indirectly increased species' antitelechorous potential through increasing dry and wet
304 dislodgement force, rather than directly affecting time to dislodgement ($\Delta LOOIC$ = 16). Through
305 both increasing dry and wet dislodgement force, a one *SD* increase in log mucilage mass
306 corresponded to a staggering 280-times increase in time to dislodgement, an effect which far
307 overshadowed other seed traits in relative importance (Figure 6B). Both mucilage wetting speed
308 and the rate of mucilage decay also had a positive indirect effect on time to dislodgement
309 through increasing wet dislodgement force, although the magnitude of their effect was
310 comparatively minor (<10% the effect size of mucilage mass). Holding mucilage mass constant,
311 seeds with a higher mass had a large negative indirect association with time to dislodgement
312 through lower dry dislodgement force. A one *SD* higher seed mass was associated with a 66%
313 reduction in antitelechorous potential through lower dry dislodgement force. The best model also
314 included a direct path from seed mass to time to dislodgement ($\Delta LOOIC$ = 22), but the weak

315 negative effect was not distinguishable from zero (β = -0.19 ± 0.15, CI_{95} = [-0.49, 0.10]). At
316 mean flow speed, the modified drag coefficient had a significant negative effect on time to
317 dislodgement in the SEM, roughly equivalent in magnitude as wet dislodgement force. However,
318 the modified drag coefficient was not affected by the amount of mucilage of the species. In
319 contrast, while seed mucilage mass substantially increased mean projected seed area, mucilage
320 mass ultimately did not indirectly reduce time to erosion to because the effect of mean projected
321 seed area is not distinguishable from zero.

322 *Marginal utility of functional assays*

323 Stepwise cross-validation revealed that including dry dislodgement force was sufficient
324 to achieve roughly three-quarters of the predictive performance of the best model containing dry
325 dislodgement force, k_d, wet dislodgement force, and mean projected area (Figure S4). Including
326 the next best variable k_d brings the model's predictive performance up to 93% of the best model.

327 **Discussion**

328 Through explicitly testing our model of the physical mechanisms at play, we
329 demonstrated that mucilage mass was by far the most important trait that affects mucilage-
330 mediated antitelechory and that it acts by increasing the force necessary for dislodgement. Thus,
331 we suggest dry dislodgement force assay as a simple proxy for mucilage-mediated antitelechory
332 in future studies, as this measurement had approximately 75% of the predictive power of the best
333 model. Our mechanistic model, based on dislodgement force and fluid resistance, explained time
334 to dislodgement extremely well (R^2 = 0.71). Thus, this model (Figure 6A) is a useful heuristic to
335 employ in further investigations of substrate attachment. We do not mean to suggest that other
336 unmeasured variables (e.g. seed surface characteristics, mucilage composition, and mucilage
337 structure) do not contribute meaningfully; rather, the basic measurements we performed are

338 sufficient to capture the vast majority of the relative antitelechory potential of across a diversity
339 of plants.

340 *What drives dislodgement force?*

341 Dislodgement force, especially that of dried mucilage was the most important predictor
342 of erosion resistance (Dried mucilage: partial R^2 = 0.26, CI_{95} = [0.00012, 0.50], Wet mucilage:
343 partial R^2 = 0.076, CI_{95} = [-0.094, 0.31]). It correlated strongly with mucilage mass, a result we
344 also found with a different set of species and a slightly different dislodgement assay (Pan et al.,
345 2021), suggesting that increased dislodgement force can be driven by simply increasing mucilage
346 production. Mucilage mass may be quite variable among close relatives (Table S2). A
347 particularly striking example occurred within *Dracocephalum* (Lamiaceae). An ornamental
348 variety of *D. moldavica* had 39 mg of mucilage in a large envelope around the nutlet and a
349 dislodgement force of > 2 N, while the similarly sized nutlets of *D. parviflorum* had < 1 mg of
350 mucilage localized in small projections at one end, and an unmeasurably small dislodgement
351 force (scored as 0.0098 N in this analysis).

352 However, considering mucilage mass as the primary predictor is overly simplistic; other
353 factors, probably composition and seed shape, are likely to contribute to dry dislodgement force.
354 The pectic mucilage of *Linum* spp., rich in rhamnogalacturonan and arabinoxylan with unusual
355 side group substitutions, provides a good example (Naran et al., 2008). Dry and wet
356 dislodgement force of Linaceae was consistently underpredicted by mucilage mass, suggesting
357 that this mucilage composition may be stronger than other types (also suggested by Kreitschitz et
358 al., 2021a). In contrast, seeds of species of Polemoniaceae were more weakly attached than
359 expected given their mucilage mass; their mucilage composition and primary function of
360 mucilage in nature is thus far unknown but deserves more investigation. We have found that it

provides a defensive benefit to several species in the family (LoPresti et al., 2019, Pan et al., 2021), though it was not as protective as mucilage of other families in those studies as well.

The substrate that seeds attach to is also important. We measured dried mucilage dislodgement force on glass microscope slides for maximum replicability. However, when testing substrates for this experiment, we found that seeds that were attached to increasingly finer grit sandpaper dislodged with less force (unpublished data). Fortunately, the glass slide assay was a good proxy for the performance on the tiles, as evidenced by its high explanatory power, although there could be realistic substrates where it is far less applicable. Drying speed also alters dislodgement force and mucilage structure (personal observations), though it is unclear how this interacts with substrate, and therefore deserving of increased scrutiny. How mucilage mass, seed shape, and mucilage composition change dislodgement force across substrate types and environmental conditions are entirely unexplored questions that could increase ecological realism in future studies of mucilage-mediated antitelechory.

Why was drag a less important predictor?

Surprisingly, the drag coefficient, despite being a significant effect, was a relatively poor predictor of time to dislodgement in our study (partial R^2 = 0.085, CI_{95} = [-0.044, 0.27]). There are both theoretical and methodological explanations for this result. It is likely that for most seeds in the most realistic erosive conditions (i.e. not our highest flow rates), drag is not sufficient to overcome the attachment potential to the substrate. Our estimates, derived from seeds falling at terminal velocity in a water-filled cylinder, also may not properly reflect the flow regime or mucilage envelope dynamics during erosive conditions. Additionally, values were probably inaccurate, though we believe that they reasonably reflect relative species differences in this study. The mucilage envelope probably deforms to a much higher extent in higher flow rates

and outer layers may shear off (Figure 3B-C), thereby reducing drag below our estimates. Further, in higher and more turbulent flow regimes, theory predicts the drag coefficient rapidly decays (White, 1991), thus contributing a lesser extent to the overall drag. As such, that the effect of the modified drag coefficient was strongest at lower flow rates was hardly surprising. Deeper investigation into this matter is beyond the scope of this study and more complex drag dynamics are surely at play than were considered here. For instance, in field pilot trials, the attached seeds caught debris during times of surface flow which surely affected the seeds' fluid resistance (Figure 3D-E). Finally, the poor explanatory performance of mean projected seed area might be attributed to similar causes. In addition, we noticed that water rarely flowed over the top of larger seeds except in higher surface flow conditions (Figure 3F). Thus, only a fraction of the projected area was truly interacting with water.

Why were mucilage decay and expansion rate poor predictors?

Given that the attachment potential of wet and dry mucilage differed so greatly, and that mucilage mass was an important predictor of attachment potential (Pan et al., 2021), we hypothesized that the time the mucilage envelope takes to expand and the rate of decay when submerged would be important components of our model. Yet, both were poor predictors of time to dislodgement (partial R^2_a = 0.042, CI_{95a} = [-0.064, 0.18]; partial R^2_D = 0.043, CI_{95D} = [-0.058, 0.18]). Each of these metrics varied greatly between species (Table S2). The mucilage of *Prunella grandiflora* (Lamiaceae) decayed far more quickly (18%/day) than any other species (mean: 5%/day), and some species had no measurable decay during the week-long trial. Time to 95% mucilage expansion varied greatly as well, from just three minutes in *Lobularia maritima* (Brassicaceae) to 5.5 hours in *Linum grandiflorum* (Linaceae).

We had hypothesized that mucilage decay in water would reduce wet dislodgement force and drag, chipping away the mucilage anchorage over time. However, the rate of mucilage dissolution appeared to be generally sufficiently low as to be of little importance within the span of one week. Though, because seeds often need to withstand erosive forces sporadically over months in nature (during which time the mucilage may be fed on by microbes or small invertebrates: Buse & Filser, 2014) before an adequate growing condition arrives, the compounding mucilage decay may take on a greater importance over longer time scales and in natural settings.

Similarly, we had hypothesized that mucilage expansion rate would affect antitelechorous potential by moderating the switch between the much stronger dry dislodgement force and the much weaker wet dislodgement force. However, our results suggest that either dry force or wet force was likely sufficient to anchor most species against lower flow rates. In an additional experiment, seeds with wet mucilage that were not allowed time to dry remained equally resistant to erosion as seeds that were and the length of mucilage drying time did not explain time to erosion (see supplement). Considering that mucilage expansion speed may increase wet dislodgement force (Figure 6A), its possible role in facilitating more rapid onset of mucilage-mediated antitelechory, even in situations of limited moisture exposure time (e.g. morning dew), may be critical in nature, but is unevaluated in this study.

Potential adaptive significance

In conditions where antitelechory is adaptive (Ellner & Schmida, 1981), seeds need to anchor using the mucilage layer only until they germinate and begin root growth. Thus, time to erosion (t_E) for a given seed can only be understood ultimately in light of its time to germination (t_G), with success defined as:

$$\frac{t_E}{t_G} > 1$$

Accordingly, for species that germinate quickly, lower anchorage ability need not be an indictment of the ability of the species to colonize highly erosive environments or the efficacy of the species' antitelochorous mechanisms. Similarly, for species with a wider germination window, effective antitelechory may require better anchorage ability.

Antitelechory, though probably an important function of mucilage in nature (Garcia-Fayos et al., 2013, Engelbrecht et al., 2014), also cannot be understood in isolation, as seed mucilage is a highly multi-functional trait. Some of the characteristics that we measured here have been demonstrated to contribute to other beneficial functions of mucilage (e.g. mucilage mass correlates with germination under water stress conditions: Teixeira et al., 2020; dry dislodgement force correlates with resistance to granivory: Pan et al., 2021). Additionally, it is reasonable, though as of yet untested, that these same traits contribute more to other functions: wet dislodgement force probably drives epizoochorous dispersal (Ryding, 2001), a slower mucilage decay rate may increase survival of seeds through the gut of herbivores (Kreitschitz et al. 2021a), and faster imbibition rate could lead to better DNA repair during brief wetting periods (Huang et al., 2008).

To understand the drivers of mucilage evolution would require a more comprehensive sampling of species and more extensive measurement of traits that uniquely account for the many alternative functional hypotheses. Increasingly finer mechanistic understanding of the seed and mucilage traits that predict specific ecological functions would create more opportunities for teasing apart the evolutionary drivers of those traits, and myxodiaspory more broadly. Short of experimentally testing real time mucilage evolution, such an effort would be necessary for causal inference of mucilage evolution and selection pressures.

Conclusion

Across a wide diversity of species, attachment of seeds to substrates with seed mucilage mediates antitelechory by increasing surface dislodgement force, facilitating seed anchorage in highly erosive environments. Mucilage binding to surfaces was a highly effective form of antitelechory regardless of its hydration status. How this antitelechory potential ultimately translates to the more ecologically meaningful seedling establishment in erosive environments probably depends greatly on both the speed of germination and the local surface flow intensity and represents an important next step in these investigations.

Our investigation into the mechanistic underpinnings demonstrated the relationship between mucilage mass and dislodgement force as pivotal in understanding the mechanistic basis of mucilage-mediated antitelechory. In contrast, our functional hypotheses about mucilage decay rate, expansion rate, and drag were largely unsupported. Nevertheless, the mucilage assays used and developed in this study should be extremely useful for future studies delving into different mucilage functional investigations. We specifically designed the assays to be cheap, simple, and replicable. In particular, in addition to its utility predicting defense against granivores (Pan et al., 2021), dry dislodgement force is a quick and informative assay to make when one seeks to obtain a rough heuristic of antitelechorous potential across a wide range of species.

Acknowledgements

The USDA ARS GRIN program provided some of the seeds and were very prompt and helpful in coordination and shipment; special thanks to Jeffrey Carstens, Tiffany Fields, and Alex Sanchez. The computing for this project was performed at the High Performance

Computing Center at Oklahoma State University supported in part through the National Science Foundation grant OAC-1531128. We thank Jesse Schafer, head of operations, who was tremendously helpful in speeding up our script. We also thank Bill Henley and Andrew Doust for sharing their lab space for us to run our experiment, John Pan for providing technical guidance on fluid mechanics, the Wetzel lab and Rick Karban for providing manuscript feedback, and Mark Fishbein for both sharing sinks and commenting on our manuscript. VSP is supported by the Early Start fellowship from Michigan State University. EFL is supported by startup funds from Oklahoma State University.

References

Aerts R, Maes W, November E, Behailu M, Poesen J, Deckers J, Hermy M, Muys B. 2006. Surface runoff and seed trapping efficiency of shrubs in a regenerating semiarid woodland in northern Ethiopia. *CATENA* 65: 61–70.

Bell T, Freckleton RP, Lewis OT. 2006. Plant pathogens drive density-dependent seedling mortality in a tropical tree. *Ecology Letters* 9: 569–574.

Bürkner P-C. 2017. brms: An R Package for Bayesian Multilevel Models Using Stan. *Journal of Statistical Software* 80: 1–28.

Bürkner P-C. 2018. Advanced Bayesian Multilevel Modeling with the R Package brms. *The R Journal* 10: 395–411.

Buse T, Filser J. 2014. Mucilaginous seeds and algal diets attract soil Collembola in preference tests. *European Journal of Soil Biology* 65: 1–6.

Cowley JM, Burton RA. 2021. The goo-d stuff: *Plantago* as a myxospermous model with modern utility. *New Phytologist* 229: 1917–1923.

Cowley JM, O'Donovan LA, Burton RA. 2021. The composition of Australian *Plantago* seeds highlights their potential as nutritionally-rich functional food ingredients. *Scientific Reports* 11: 12692.

Ellner S, Shmida A. 1981. Why are adaptations for long-range seed dispersal rare in desert plants? *Oecologia* 51: 133–144.

Engelbrecht M, Bochet E, García-Fayos P. 2014. Mucilage secretion: an adaptive mechanism to reduce seed removal by soil erosion?: Mucilage Secretion and Seed Removal. *Biological Journal of the Linnean Society* 111: 241–251.

Fuller PJ, Hay ME. 1983. Is Glue Production by Seeds of Salvia Columbariae a Deterrent to Desert Granivores? *Ecology* 64: 960–963.

Goodrich B, Gabry J, Ali I, Brilleman S (2020). "rstanarm: Bayesian applied regression modeling via Stan." R package version 2.21.1, https://mc-stan.org/rstanarm.

García-Fayos P, Engelbrecht M, Bochet E. 2013. Post-dispersal seed anchorage to soil in semiarid plant communities, a test of the hypothesis of Ellner and Shmida. *Plant Ecology* 214: 941–952.

Gelman A, Goodrich B, Gabry J, Vehtari A. 2019. R-squared for Bayesian Regression Models. *The American Statistician* 73: 307–309.

Grubert M. 1974. Studies on the distribution of myxospermy among seeds and fruits of Angiospermae and its ecological importance. *Acta Biologica Venezuelica* 8: 315–551.

Grubert M. 1981. Mucilage Or Gum in Seeds and Fruits of Angiosperms: A Review. Minerva-Publikation.

Han L, Jiao J, Jia Y, Wang N, Lei D, Li L. 2011. Seed removal on loess slopes in relation to runoff and sediment yield. *CATENA* 85: 12–21.

Huang Z, Boubriak I, Osborne DJ, Dong M, Gutterman Y. 2008. Possible Role of Pectin-containing Mucilage and Dew in Repairing Embryo DNA of Seeds Adapted to Desert Conditions. *Annals of Botany* 101: 277–283.

Huang D, Wang C, Yuan J, Cao J, Lan H. 2015. Differentiation of the seed coat and composition of the mucilage of Lepidium perfoliatum L.: a desert annual with typical myxospermy. *Acta Biochimica et Biophysica Sinica* 47: 775–787.

Inceer H. 2011. Achene slime content in some taxa of Matricaria L. (Asteraceae). *Acta Botanica Croatica* 70.

Jin Y, Qian H. 2019. V.PhyloMaker: an R package that can generate very large phylogenies for vascular plants. *Ecography* 42: 1353–1359.

Kim TN, Underwood N. 2015. Plant neighborhood effects on herbivory: damage is both density and frequency dependent. *Ecology* 96: 1431–1437.

Kreitschitz A, Kovalev A, Gorb SN. 2015. Slipping vs sticking: Water-dependent adhesive and frictional properties of Linum usitatissimum L. seed mucilaginous envelope and its biological significance. *Acta Biomaterialia* 17: 152–159.

Kreitschitz A, Gorb SN. 2018. The micro- and nanoscale spatial architecture of the seed mucilage—Comparative study of selected plant species. *PLOS ONE* 13: e0200522.

Kreitschitz A, Haase E, Gorb SN. 2021a. The role of mucilage envelope in the endozoochory of selected plant taxa. *The Science of Nature* 108: 2.

Kreitschitz A, Kovalev A, Gorb SN. 2021b. Plant Seed Mucilage as a Glue: Adhesive Properties of Hydrated and Dried-in-Contact Seed Mucilage of Five Plant Species. *International Journal of Molecular Sciences* 22: 1443.

Kreitschitz A, Vallès J. 2007. Achene morphology and slime structure in some taxa of Artemisia L. and Neopallasia L. (Asteraceae). *Flora - Morphology, Distribution, Functional Ecology of Plants* 202: 570–580.

LoPresti EF, Pan V, Goidell J, Weber MG, Karban R. 2019. Mucilage-bound sand reduces seed predation by ants but not by reducing apparency: a field test of 53 plant species. *Ecology* 100: e02809.

Loudon C, Zhang J. 2002. Measuring drag without a force transducer: a terminal velocity assay. *Functional Ecology* 16: 268–272.

Mennan H, Zandstra BH. 2006. The Effects of Depth and Duration of Seed Burial on Viability, Dormancy, Germination, and Emergence of Ivyleaf Speedwell (Veronica hederifolia). *Weed Technology* 20: 438–444.

Naran R, Chen G, Carpita NC. 2008. Novel Rhamnogalacturonan I and Arabinoxylan Polysaccharides of Flax Seed Mucilage. *Plant Physiology* 148: 132–141.

North HM, Berger A, Saez-Aguayo S, Ralet M-C. 2014. Understanding polysaccharide production and properties using seed coat mutants: future perspectives for the exploitation of natural variants. *Annals of Botany* 114: 1251–1263.

Pan VS, McMunn M, Karban R, Goidell J, Weber MG, LoPresti EF. Mucilage-binding to ground protects seeds of many plants from harvester ants: a functional investigation. *Functional Ecology* In press.

Poulain D, Botran L, North HM, Ralet M-C. 2019. Composition and physicochemical properties of outer mucilage from seeds of Arabidopsis natural accessions. *AoB PLANTS* 11.

Qian H, Jin Y. 2016. An updated megaphylogeny of plants, a tool for generating plant phylogenies and an analysis of phylogenetic community structure. *Journal of Plant Ecology* 9: 233–239.

Qiu Y-L, Li L, Wang B, Xue J-Y, Hendry TA, Li R-Q, Brown JW, Liu Y, Hudson GT, Chen Z-D. 2010. Angiosperm phylogeny inferred from sequences of four mitochondrial genes. *Journal of Systematics and Evolution* 48: 391–425.

R Core Team. 2020. *R: A language and environment for statistical computing.* Vienna, Austria: R Foundation for Statistical Computing.

Roberts DR, Bahn V, Ciuti S, Boyce MS, Elith J, Guillera-Arroita G, Hauenstein S, Lahoz-Monfort JJ, Schröder B, Thuiller W, *et al.* 2017. Cross-validation strategies for data with temporal, spatial, hierarchical, or phylogenetic structure. *Ecography* 40: 913–929.

de Rouw A, Ribolzi O, Douillet M, Tjantahosong H, Soulileuth B. 2018. Weed seed dispersal via runoff water and eroded soil. *Agriculture, Ecosystems & Environment* 265: 488–502.

Smith SA, Brown JW. 2018. Constructing a broadly inclusive seed plant phylogeny. *American Journal of Botany* 105: 302–314.

Teixeira A, Iannetta P, Binnie K, Valentine TA, Toorop P. 2020. Myxospermous seed-mucilage quantity correlates with environmental gradients indicative of water-deficit stress: Plantago species as a model. *Plant and Soil* 446: 343–356.

USDA Agricultural Research Service. (2015). Germplasm Resources Information Network (GRIN). Ag Data Commons. Accessed 2021-02-09.

Vehtari A, Gabry J, Magnusson M, Yao Y, Gelman A. 2019. Efficient LOO-CV and WAIC for Bayesian models — loo-package.

Vehtari A, Gelman A, Gabry J. 2017. Practical Bayesian model evaluation using leave-one-out cross-validation and WAIC. *Statistics and Computing* 27: 1413–1432.

Veiga-Barbosa L, Pérez-García F, Veiga-Barbosa L, Pérez-García F. 2014. Germination of mucilaginous seeds of Plantago albicans (Plantaginaceae): effects of temperature, light, pre-sowing treatments, osmotic stress and salinity. *Australian Journal of Botany* 62: 141–149.

Vertucci CW. 1989. The Kinetics of Seed Imbibition: Controlling Factors and Relevance to Seedling Vigor. In: Seed Moisture. John Wiley & Sons, Ltd, 93–115.

Villellas J, García MB. 2013. The role of the tolerance–fecundity trade-off in maintaining intraspecific seed trait variation in a widespread dimorphic herb. *Plant Biology* 15: 899–909.

Viudes S, Burlat V, Dunand C. 2020. Seed mucilage evolution: Diverse molecular mechanisms generate versatile ecological functions for particular environments. *Plant, Cell & Environment* 43: 2857–2870.

Western TL. 2012. The sticky tale of seed coat mucilages: production, genetics, and role in seed germination and dispersal. *Seed Science Research* 22: 1–25.

White FM. 1991. *Viscous Fluid Flow*. McGraw-Hill.

Zanne AE, Tank DC, Cornwell WK, Eastman JM, Smith SA, FitzJohn RG, McGlinn DJ, O'Meara BC, Moles AT, Reich PB, *et al.* 2014. Three keys to the radiation of angiosperms into freezing environments. *Nature* 506: 89–92.

Zhou Z, Xing J, Zhao J, Liu L, Gu L, Lan H. 2021. The ecological roles of seed mucilage on germination of Lepidium perfoliatum, a desert herb with typical myxospermy in Xinjiang. *Plant Growth Regulation* In press.

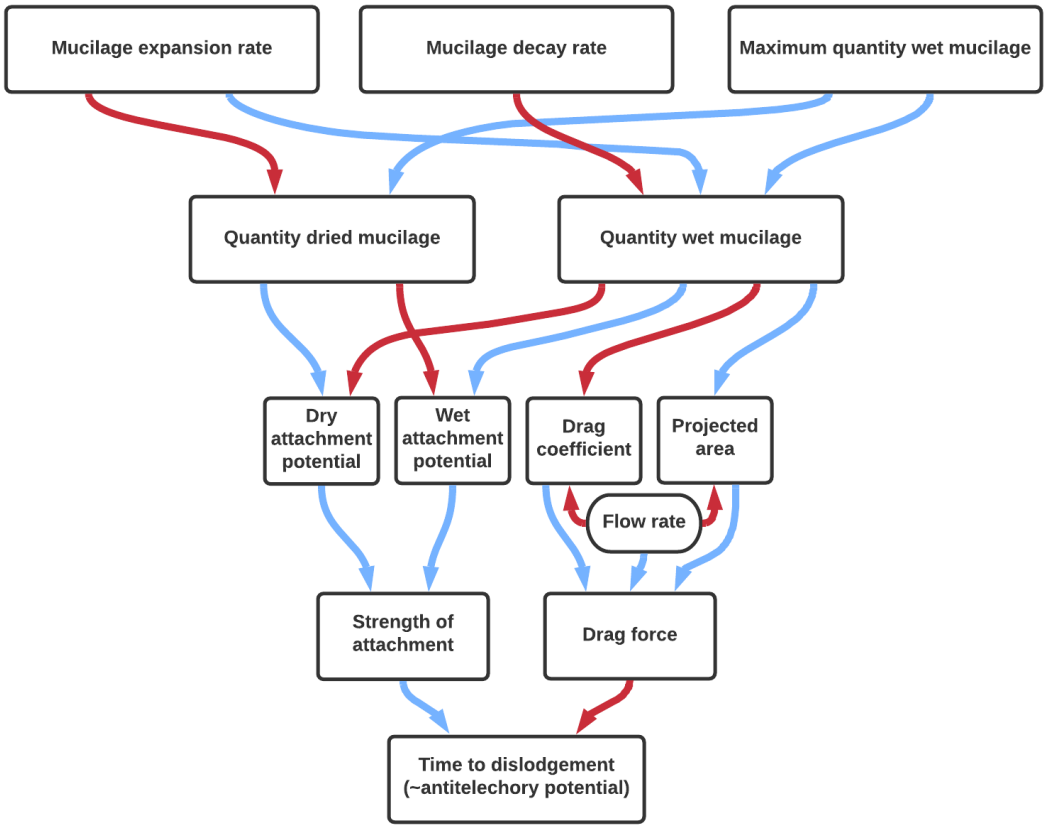

Figure 1. Diagram illustrating the hypothetical ways that mucilage traits may mechanistically influence antitelechory. Red arrows represent a negative effect, whereas blue arrows represent a positive effect.

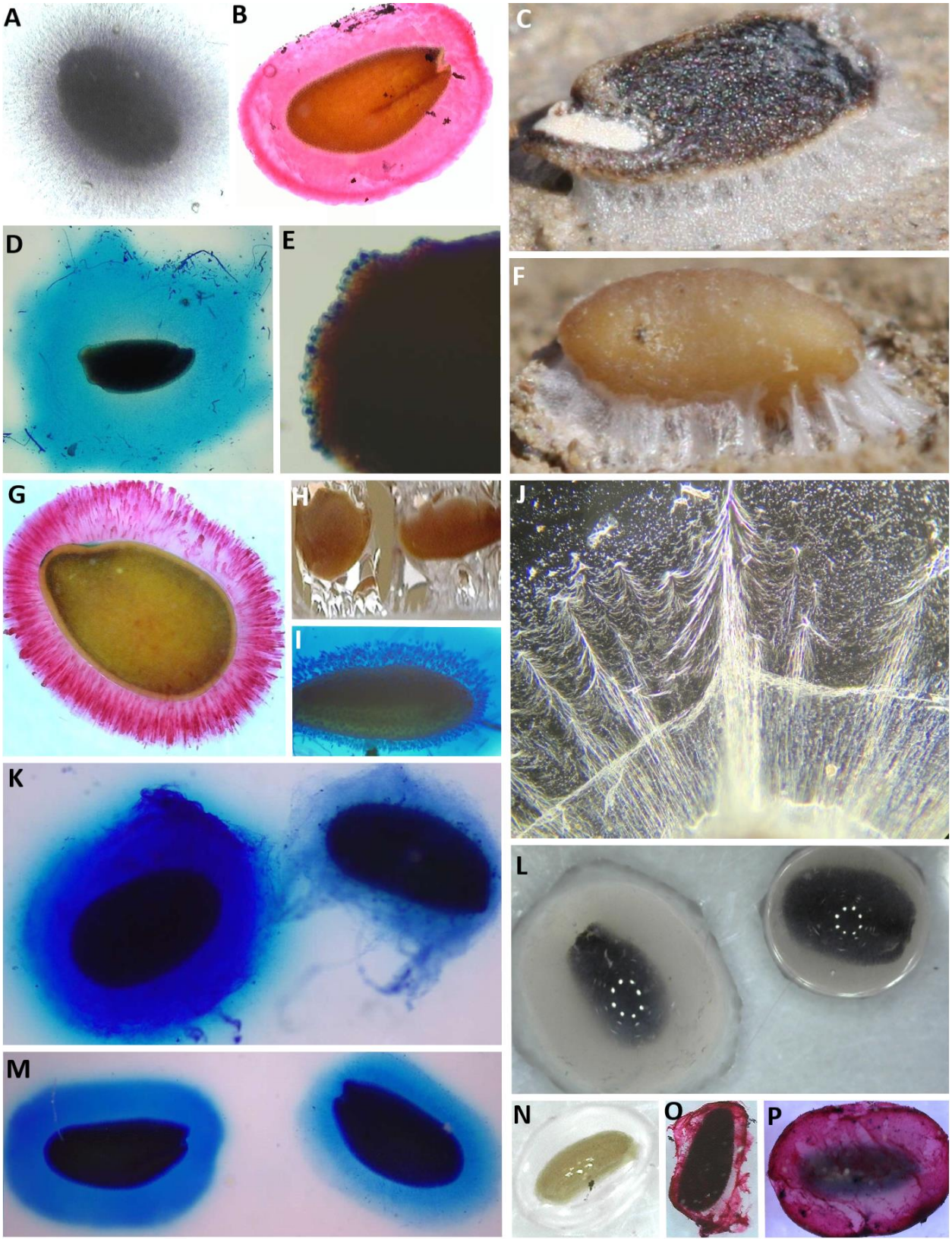

Figure 2. (A) *Ocimum basilicum* (Lamiaceae) with visible starch granules stained with Lugol's iodine. (B) *Lepidium sativum* (Brassicaceae), (G) *Linum grandiflornum* (Linaceae), (O) *Melissa officinalis* (Lamiaceae), and (P) *Salvia coccinea* (Lamiaceae) stained with Ruthenium red that to show different mucilage structures based on distributions of pectic sugars.

(I) *Plantago* (Plantaginaceae) seeds, pictured: *P. patagonica*, takes many times longer to fully expand their mucilage than (N) *Matricaria chamomilla* (Asteraceae) achenes. Seed mucilage also varies in quantity and projected area: (D) *Dracocephalum moldavica* (Lamiaceae) and (E) *D. parviflorum* both stained with methylene blue show different interspecific mucilage volume. (L) two unstained *O. basilicum* nutlets from the same batch show different intraspecific mucilage volumes. Mucilage decay due to extended imbibition affects mucilage quantity: (K) *S. hispanica* and (M) *Le. sativum* stained with methylene blue. The seeds on the right that were imbibed for 12 days had a thinner mucilage envelope compared to the seeds on the left that were imbibed for an hour. The attachment potential of mucilage depends on its hydration status: (C) *D. moldavica* and (F) *Gilia leptantha* (Polemoniaceae) dried mucilage strongly cemented on soil surface. (J) *Le. sativum* dried mucilage magnified under phase contrast. (H) *Li. grandiflorum* wet mucilage stretching apart by two pieces of filter paper. Staining methodology adapted from (Kreitschitz et al., 2021b)

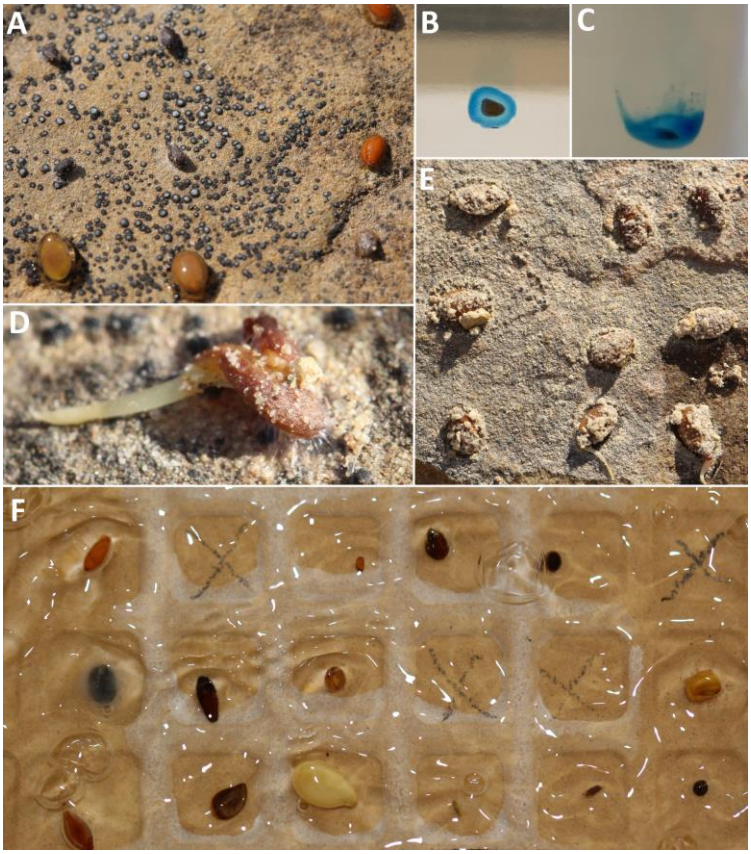

Figure 3. (A) Imbibed seeds with wet mucilage drying on sandstone (*Ocimum basilicum*, four in upper left; *Lepidium sativum*, two in upper right; *Linum grandiflorum*, two in lower left; *Salvia hispanica*, lower right). (B) *Gilia tricolor* and (C) *Dracocephalum* 'blue dragon' seeds stained with methylene blue falling in water. The mucilage envelope in C can be seen deformed and shearing off as it falls, in contrast to the limited deformation in B. (D) *Le. sativum* seed attached by dried mucilage strands on sandstone in the process of elongating its radical. (E) *Li. grandiflorum* with entrapped substrates attached to sandstone in the field, after a bout of natural surface flow. (F) Seeds attached to the back side of a tile during an erosion assay (Top row, left to right: *Le. sativum, Capsella bursa-pastoris, Prunella grandiflora, Plectranthus scutellarioides*; Middle row: *O. basilicum, Plantago maritima, Eruca vesicaria, Anastatica hierochuntica*; Bottom row: *Plantago ovata, Linum perenne, Linum usitatissimum, Matricaria chamomilla, Artemisia dracunculus, Thymus vulgaris*).

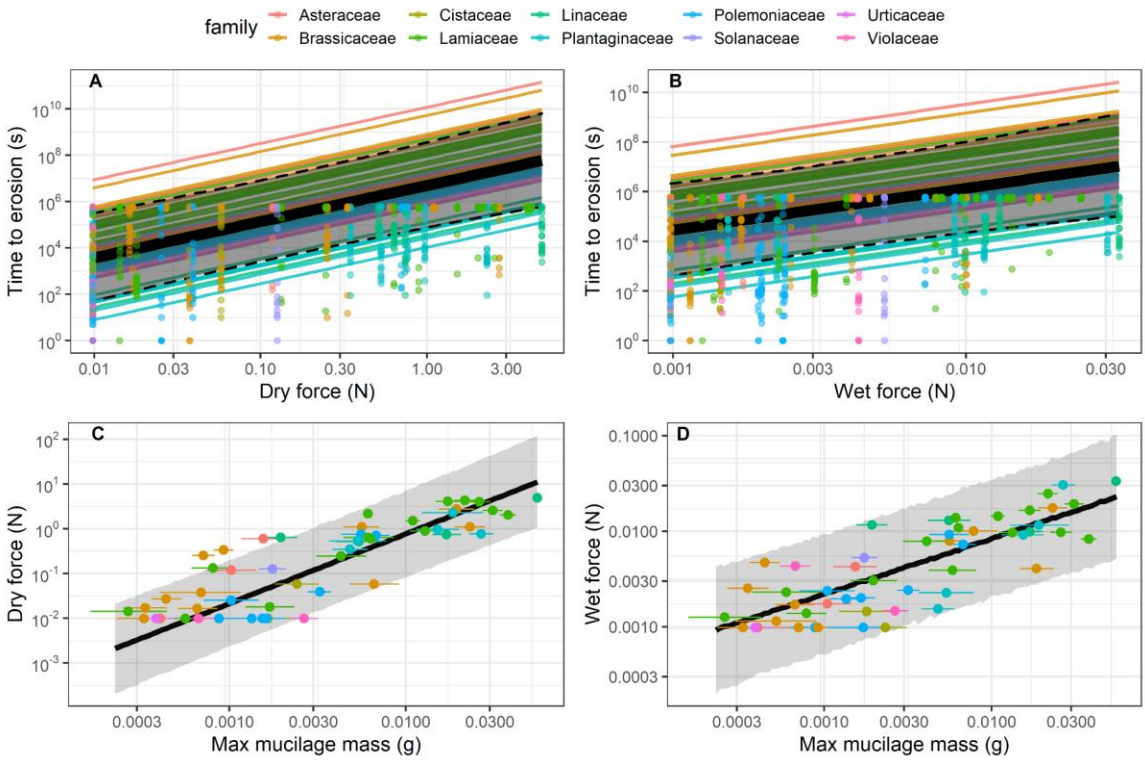

Figure 4. Relationship between time to erosion and dislodgement force (A & B) and between dislodgement force and fully imbibed mucilage mass (C & D) as predicted by a phylogenetic AFT multilevel model and two phylogenetic linear models. Black lines show the global relationship with grey ribbons representing the 95% *CIs*. Points and lines are colored by family. In A-B, species specific slopes are plotted as thinner lines. Each point corresponds to individual observed seed erosion time. In C-D, each point corresponds to imputed measurement error free mean species mucilage mass and observed mean species dislodgement force. Error bars represent 95% *CIs*.

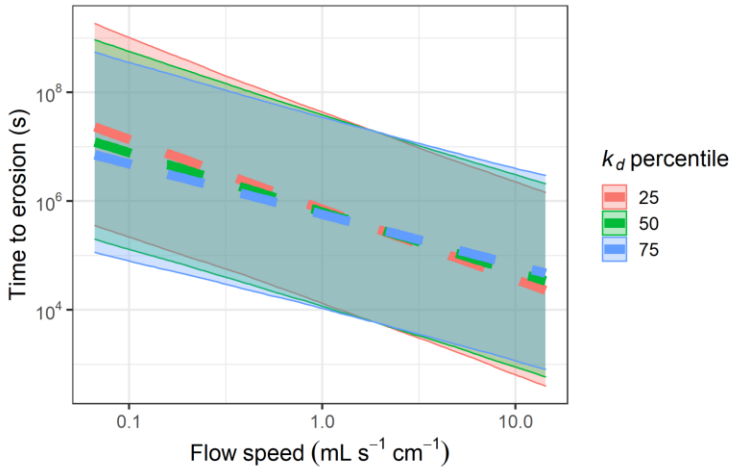

Figure 5. Effect of flow speed on time to erosion as predicted by a phylogenetic AFT multilevel model. Colors correspond to a seed with k_d value at the 25th, 50th, or 75th percentile. Dashed lines show the global trends with ribbons showing the 95% *CIs*.

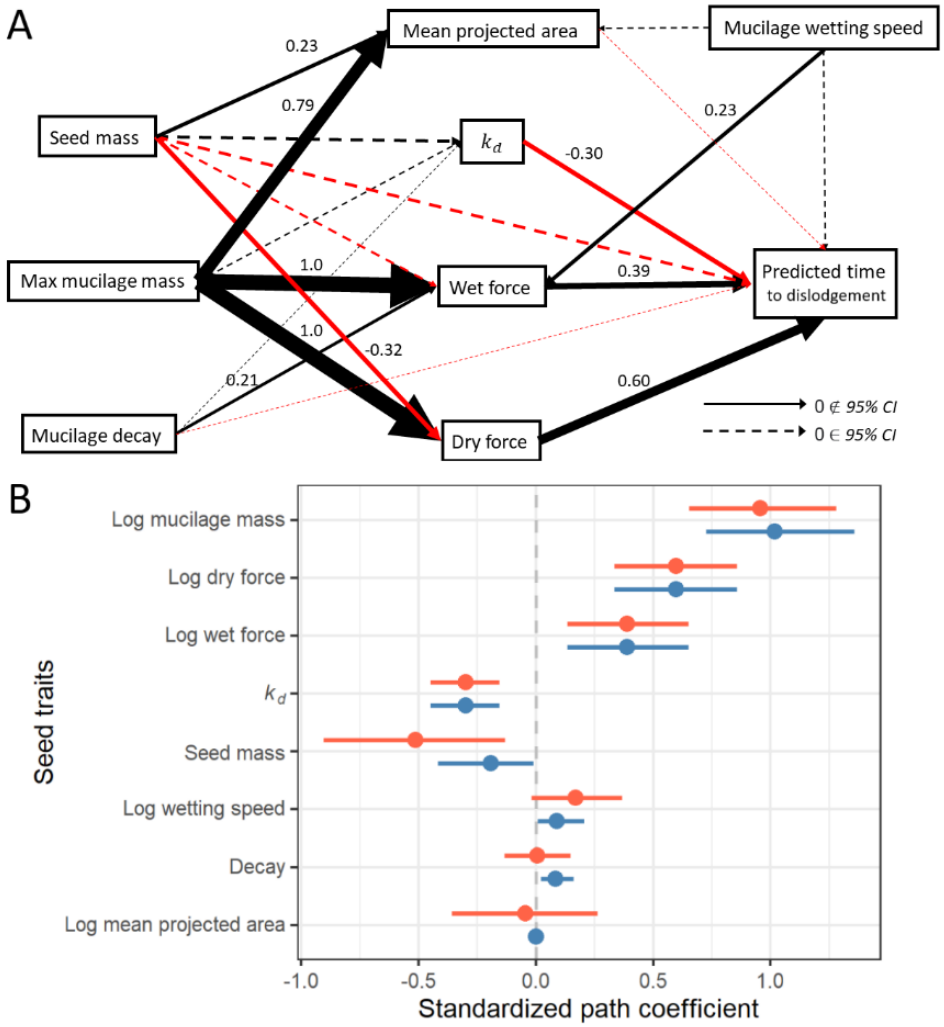

Figure 6. (A) Path diagram of the best SEM. Paths with *95% CI* overlapping with zero are indicated by dashed lines; otherwise, they are indicated by a solid line along with their corresponding standardized path coefficient. The size and color of all paths were scaled to the magnitude and direction of the effect respectively (red = negative; black = positive). A direct path from seed mass to erosion time ($\Delta LOOIC$ = 22), from wetting speed to mean projected area ($\Delta LOOIC$ = 6), and from wetting speed to wet force were added ($\Delta LOOIC$ = 23), though only the path from wetting speed to wet force was significant ($\beta = 0.23 \pm 0.10$, CI_{95} = [0.033, 0.43]). This positive association was likely because seeds that released mucilage faster had more mucilage at

the time the wet dislodgement force was measured. (B) Total effect of each seed trait on predicted log species mean erosion time. Error bars represent 95% *CIs*. Total path coefficients calculated based on all paths or only significant paths are shown in red and blue respectively. All variables besides mucilage decay rate, k_d, and seed mass are on the log scale.